ScienceDirect

Contents lists available at ScienceDirect

Journal of Iron and Steel Research, International

journal homepage: www.chinamet.cn

Elastic deformation behavior of CuZrAlNb metallic glass matrix composites with different crystallization degrees

Wei-zhong Liang[1,*], Zhi-liang Ning[2,3], Gang Wang[4], Zhi-jie Kang[1], Hai-chao Sun[2,3], Yong-sheng Chen[1]

[1] School of Materials Science and Engineering, Heilongjiang University of Science and Technology, Harbin 150022, Heilongjiang, China

[2] School of Materials Science and Engineering, Harbin Institute of Technology, Harbin 150001, Heilongjiang, China

[3] National Key Laboratory for Precision Hot Processing of Metals, Harbin Institute of Technology, Harbin 150001, Heilongjiang, China

[4] Laboratory for Microstructures, Shanghai University, Shanghai 200444, China

ARTICLE INFO

Key words:
Metallic glass matrix composite
Digital image correlation technique
Elastic deformation
Strain field

ABSTRACT

The room temperature brittleness has been a long standing problem in bulk metallic glasses realm. This has seriously limited the application potential of metallic glasses and their composites. The elastic deformation behaviors of metallic glass matrix composites are closely related to their plastic deformation states. The elastic deformation behaviors of $Cu_{48-x}Zr_{48}Al_4Nb_x$ ($x=0$, 3 at. %) metallic glass matrix composites (MGMCs) with different crystallization degrees were investigated using an in-situ digital image correlation (DIC) technique during tensile process. With decreasing crystallization degree, MGMC exhibits obvious elastic deformation ability and an increased tensile fracture strength. The notable tensile elasticity is attributed to the larger shear strain heterogeneity emerging on the surface of the sample. This finding has implications for the development of MGMCs with excellent tensile properties.

1. Introduction

Bulk metallic glasses (BMGs) have shown excellent mechanical properties[1-4], which make them ideal for structural and functional applications. However, their room temperature brittleness and strain softening behavior have significantly limited their applications[5,6]. To overcome their brittleness behavior, metallic glass matrix composites (MGMCs) by introduction of the crystalline phase into glassy matrix have been developed[7-10]. The improved tensile or compressive ductility can be attained in Ti-based[11], Zr-based[12], La-based[13], Mg-based[14] and CuZr-based[15-20] MGMCs by adjustment of compositions or cooling rates. Especially, CuZr-based MGMCs have attracted great attention owing to their strong glassy forming ability and remarkable ductile material feature. It was pointed out that the characteristics of shear bands on the fracture samples have great effect on mechanical properties of CuZr-based MGMCs. However, the relationship between the macroscopic elastic deformation of MGMCs and microscopic strain energy distribution is still not well understood.

Digital image correlation (DIC) technique provides an effective method to display the strain field evolution with stress through recording sequentially digital maps of surface features on the tested sample during deformation, and then post-processing these images based on a pattern-matching algorithm[21-23]. The DIC technique has been widely used in the investigation of BMGs[1,24], which can effectively plot the strain field distribution on the surface of BMGs. Based on the DIC observation, the strain concentration for the operation of shear banding during tensile deformation in BMGs can be quantitatively evaluated. For MGMCs, the second phase embedding into the glassy matrix should disturb the shear-banding behavior. Accordingly, the strain field before shear banding should be changed due to the second phase in MGMCs. However, so far, attention has not been paid to the strain concentration during the elastic deformation of MGMCs. Regarding this, in this study, the relationships among microscopic strain and strain energy accumulation in $Cu_{48-x}Zr_{48}Al_4Nb_x$ ($x=0$, 3 at. %) MGMCs under elastic deformation

* Corresponding author. Prof., Ph.D.
E-mail address: *wzliang1966@126.com* (*W. Z. Liang*).

Received 12 December 2016; Received in revised form 3 March 2017; Accepted 3 March 2017
Available online 15 April 2017

stages are investigated through using in-situ observation of DIC technique.

2. Experimental Procedures

Button ingots of $Cu_{48-x}Zr_{48}Al_4Nb_x$ ($x=0$, 3 at. %, denoted as 0Nb and 3Nb, respectively) alloys were fabricated by arc melting mixtures of the composing element (99.9% purity) in a Ti-gettered argon atmosphere. Alloy ingots were re-melted four times to ensure chemical homogeneity. Cylindrical rod with a diameter of 3 mm and a length of 47 mm was synthesized by drop-casting into a copper mould in a purified argon atmosphere. The structures of the 0Nb and 3Nb alloys were charactered by X-ray diffraction with CuKα radiation ($\lambda=0.15405$ nm) using a D/MAX-RB diffractometer in previous work, which revealed that both Al_2Zr and B2-CuZr crystalline phases were detected in the 0Nb alloy and that only few B2-CuZr phase appeared in the 3Nb alloy[25]. Thermal analysis was carried out by a Pyris-1 differential scanning calorimetry (DSC) at a heating rate of 0.33 K/s, which exhibited that the 0Nb alloy had larger volume fraction of the crystalline phase than that of the 3Nb alloy[25]. Tension tests were performed on a dog-bone shape samples with gauge dimensions of 10 mm×2 mm×1 mm by using an INSTRON-5569 testing machine with a strain rate of 3.45×10^{-4} s^{-1} at room temperature. The tensile specimens were spray-painted to generate an artificial speckle suitable for DIC measurement. The spray-painted sample surface was illuminated by two fibre-optic white-light sources during loading. A Charge-Coupled Device video camera with a resolution of 5 μm/pixel was used to capture the consecutive speckle images at a frequency of 4 Hz during the deformation. A rectangular 420 × 140 pixel frame located at the centre of the sample surface was selected for strain calculations. The sequential speckle images were calculated using the Newton-Raphson iteration algorithm.

3. Results and Discussion

Fig. 1 shows the tensile stress-strain curves of the $Cu_{48-x}Zr_{48}Al_4Nb_x$ ($x=0$, 3 at. %) samples at room temperature. The 0Nb sample shows typical brittle fracture with lower fracture strength of (1140±11) MPa after small elastic deformation. The 3Nb sample displays the fracture strength of (1725±15) MPa after larger elastic deformation. It is evident that the larger fracture strength and elastic deformation ability can be achieved in the 3Nb MGMCs due to the enhanced glassy forming ability.

Fig. 2(a－c) presents the surface speckle image without loading and the DIC results of the in-situ tension of the 0Nb sample. The normal strain (ε_y, along the loading direction) fields and the shear strain (γ_{xy})

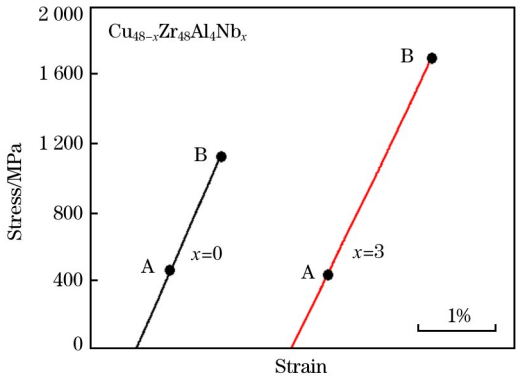

Fig. 1. Stress-strain curves of $Cu_{48-x}Zr_{48}Al_4Nb_x$ ($x=0$, 3 at. %) samples with a diameter of 3 mm.

fields recorded at different stresses are mapped in Fig. 2(b,c), respectively. In the stress range from 177 to 270 MPa, no notable strain concentration is observed in two strain fields (Fig. 2(b,c)). It can be seen that the stress approaching 393 MPa causes the strain fields to distribute inhomogeneously. The strain-concentration striations are formed in the ε_y field, and some strain-concentration regions emerge in the γ_{xy} field. When the stress is increased from 477 to 1140 MPa, the positive strain-concentration striations in the ε_y fields and the positive strain-concentration regions in the γ_{xy} fields are significantly enlarged. The angles between the positive strain-concentration striations and the loading direction are 64° in the ε_y field.

Fig. 3(a－c) presents the surface speckle image without loading and the DIC results of the in-situ tension of the 3Nb sample. ε_y and γ_{xy} fields recorded at different stresses are mapped in Fig. 3(b,c), respectively. In the stress range from 178 to 437 MPa, no notable strain concentration is observed in two fields (Fig. 3(b,c)). When the stress reaches 824 MPa, the strain-concentration striations appear in the ε_y field, and the strain-concentration regions emerge in the γ_{xy} fields. With increasing the stress from 1250 to 1687 MPa, the positive strain-concentration striations in the ε_y fields and the positive strain-concentration regions in the γ_{xy} fields also show a correspondingly sharp rise. The angles between the positive strain-concentration striations and the loading direction are 68° in the ε_y field. More strain-concentration regions are observed in 3Nb sample as compared to the cases in 0Nb sample in the γ_{xy} and ε_y fields.

It is obvious that the elastic deformation of MGMCs is tightly associated with the strain concentration. The strain distributions in two samples from the DIC images indicate that the strain-energy distributions are inhomogeneous within the strain-concentration zones, which is proved by the positive strain-concentration striations in the ε_y fields and the positive granule-